SEGMENTATION OF BLUR IMAGES USING LOCAL BINARY PATTERN TECHNIQUE

Kavadapu Mounika (M.Tech(CSP))1
M.Devendra (M.S.,(Ph.D))2, Associate Professor2
Department of Electronics and Communication Engineering1,2
G.Pulla Reddy Engineering College (Autonomous), Kurnool, Andhra Pradesh,India1,2
kavadapumounika452@gmail.com1   devendragprecece@gmail.com2

Abstract

Defocus blur is to a great degree regular in images caught utilizing optical imaging frameworks. It might be bothersome, however may likewise be a deliberate imaginative impact, in this manner it can either upgrade or hinder our visual view of the image scene. For assignments, for example, image restoration and object recognition, one should need to portion an in part blurred image into blurred and non-blurred areas. In this paper, we propose sharpness metric in light of local binary patterns and a hearty segmentation calculation to isolate all through focus image districts. The proposed sharpness metric adventures the perception that most local image fixes in blurry areas have altogether less of certain local binary patterns contrasted and those in sharp districts. Utilizing this metric together with image tangling and multiscale surmising, we got excellent sharpness maps. Tests on several halfway blurred images were utilized to assess our blur segmentation calculation and six comparator techniques. The outcomes demonstrate that our calculation accomplishes similar segmentation comes about with the best in class and have enormous speed advantage over the others. in Extension we are using LLBP (Line Local Binary Pattern) for getting better output in blur images.

Index Terms— Defocus, blur, segmentation, LBP, local binary patterns, image restoration, object recognition, out-of-focus, blurred.

I.INTRODUCTION

DEFOCUS obscure in a picture is the aftereffect of an out-of-center optical imaging framework. In the Picture arrangement process, light transmitting from focuses on the concentration plane are mapped to a point in the sensor, however light from a point outside the concentration plane enlightens a non-point area on the sensor known as a hover of perplexity. Defocus obscure happens when this circle turns out to be sufficiently vast to be seen by human eyes. In computerized photography, defocus obscure is utilized to obscure foundation and "fly out" the principle subject utilizing vast opening focal points. Nonetheless, this represses computational picture understanding since obscuring of the foundation smothers points of interest helpful to scene elucidation.

For this situation, partition of the obscured and sharp districts of a picture might be fundamental so post-handling or rebuilding calculations can be connected without influencing the sharp areas, or so picture highlights are just removed from in-center locales. Most present picture deblurring techniques accept that the obscure is spatially invariant [1]. Normally, a worldwide obscure portion is evaluated and the first picture is remade by fitting it to various picture priors with maximum a posteriori estimation. Strategies that unequivocally display spatially variation obscure commonly reestablish little picture fixes inside which

obscure can be dealt with as invariant, and reestablished patches are sewed together [2], [6], [10].

Productive and exact discovery of obscured or non-obscured districts is valuable in a few settings including:

1) In dodging costly post-preparing of non-obscured areas (e.g. deconvolution) [10];

2) In computational photography to distinguish an obscured foundation and further obscure it to accomplish the imaginative bokeh impact [2], [3], especially for high-profundity of-field PDA cameras; and

3) for question acknowledgment in spaces where objects of intrigue are not in with no reservations center (e.g. microscopy pictures) and parts of the question which are obscured must be recognized to guarantee legitimate extraction of picture highlights, or, if just the foundation is obscured, to fill in as an extra prompt to find the frontal area protest and perform question driven spatial pooling [10].

Thus, this issue is expressly tended to without measuring the degree of fogginess and sharpness metric in light of Local Binary Patterns (LBP) is presented.

II. RELATED WORKS

The most regularly observed approach for defocus division writing is by means of neighborhood sharpness estimation. There are numerous works around there in the previous two decades and the majority of them can be found in the picture quality appraisal field where pictures are evaluated by a solitary sharpness score that should fit in with the

human visual discernment. These applications just require a solitary sharpness incentive to be accounted for a solitary picture, in this manner the vast majority of the measures just depend on sharpness around neighborhood edges [4] or some particular picture structures decided in the mind boggling wavelet change space [7].

Also, the line spread profile has been embraced for edge haziness estimation in picture recover identification [6]. Since the greater part of these measurements are estimated around edges, they can't promptly describe sharpness of any given neighborhood picture content except if edge-sharpness is interjected somewhere else as was done in [4] and [7]. Measures, for example, higher request insights [10], difference of wavelet coefficients [2], neighborhood fluctuation picture field [3] have been utilized straightforwardly in division of objects of enthusiasm for low-profundity of-field pictures. These neighborhood sharpness measurements depend on nearby picture vitality which implies that the measures won't just diminishing if the vitality of the PSF (point spread capacity) diminishes (turns out to be more hazy), yet additionally diminishes if the vitality of the picture content drops. Hence, a hazy, high-differentiate edge area could have a higher sharpness score than an in-concentrate, low-differentiate one.

As of late, Liu et al. [2] and Shi et al. proposed an arrangement of novel nearby sharpness highlights, e.g. slope histogram traverse, kurtosis, for preparing of a gullible Bayes classifier for obscure arrangement of neighborhood picture districts. The sharpness is translated as the probability of being named sharp fix. Su et al. utilized solitary esteem decay (SVD) of

picture highlights to portray obscure and basic thresholding for obscured area location [10].

Vu et al. utilized nearby power range slant and neighborhoods add up to variety for the measure in both the ghostly and spatial areas. The last sharpness is the geometric mean of the two measures [5]. Rather than estimating sharpness just in view of nearby data, Shi et al. proposed to take in a meager word reference in light of a huge outside arrangement of defocus pictures and after that utilization it to assemble an inadequate portrayal of the test picture fix. The last measure was the quantity of non-zero components of the comparing words [10]. Profundity delineate is another approach that can likewise be utilized for defocus obscure division.

Zhuo et al. utilized edge width as a kind of perspective for profundity estimation under the supposition that edges in obscured areas are more extensive than those in sharp locales [7]. They got a persistent defocus delineate proliferating the sharpness measures at edges to whatever is left of the picture utilizing picture tangling [10]. Bae and Durand's work is comparative, yet they figured edge width distinctively by finding the separation of second subordinate extrema of inverse sign in the inclination bearing [4]. These strategies tend to feature edges in places where the obscure measure is really smooth.

Zhu et al. endeavored to unequivocally appraise the space-variation PSF by breaking down the confined recurrence range of the slope field [6]. The defocus obscure piece is parameterized as an element of a solitary variable (e.g. sweep for a circle portion or change for Gaussian part) and is assessed by means of MAPk estimation. Comparable work can be found in [9] however the obscure piece is confined to a

limited number of hopefuls. Khosro et al. evaluate the obscure piece locally through visually impaired picture deconvolution by accepting the portion is invariant inside the nearby square. Be that as it may, rather than fitting the assessed part to a parameterized display, they quantized the sharpness through reblurring [5].

A. Gradient Domain Metrics

1) Gradient Histogram Span :

The gradient magnitude of sharp images exhibits a heavy-tailed distribution [1], [2] and can be modeled with a two component Gaussian mixture model (GMM):

$$G = a_1 e^{-\frac{(g-\mu_1)^2}{\sigma_1}} + a_2 e^{-\frac{(g-\mu_2)^2}{\sigma_2}} \quad (1)$$

Where means $\mu_1 = \mu_2 = 0$, variance $\sigma_1 > \sigma_2$, g is the gradient magnitude, and G is the gradient magnitude distribution in a local region. The component with larger variance is believed to be responsible for the heavy-tailed property. Thus the local sharpness metric is:

$$m_{GHS} = \sigma_1 \quad (2)$$

2) Kurtosis :

Kurtosis, which captures the "peakedness" of a distribution, also characterizes the gradient magnitude distribution difference. It is defined as:

$$k = \frac{E[(g-\mu)^4]}{E^2[(g-\mu_1)^2]} - 3 \quad (3)$$

Where the first term is the fourth moment around the mean divided by the square of the second moment around the mean. The offset of 3 is to cause the

peakedness measure of a normal distribution to be 0. The derived local sharpness metric is:

$$m_K = \min\left(ln(K(g_x) + 3), ln(K(g_y) + 3)\right) (4)$$

Where g_x, g_y are gradient magnitudes along x and y axis respectively.

B. Intensity Domain Metrics

1) Singular Value Decomposition (SVD) :

An image patch P can be decomposed by SVD:

$$P = U \Lambda V^T = \sum_{i=1}^{n} \lambda_i u_j v v_i^T (5)$$

where U,V are orthogonal matrices, is a diagonal matrix whose diagonal entries are singular values arranged in descending order, u_i and v_i are the column vectors of U and V respectively, and λ_i are the singular values of. It is claimed that large singular values correspond to the rough shape of the patch whereas small singular values correspond to details. The sharpness metric is:

$$m_{SVD}(k) = 1 - \frac{\sum_{i=1}^{k} \lambda_i}{\sum_{i=1}^{n} \lambda_i} (6)$$

Where the numerator is the sum of the k largest singular values.

2) Linear Discriminant Analysis (LDA) :

By sampling a set of blurred and non-blurred patches, this method finds a transform W that maximizes the ratio of the between-class variance S_b to the within-class variance S_w of the projected data with each variance:

$$S_b = \sum_{j=1}^{2} (\mu j - \mu)^T (\mu j - \mu)$$

$$S_w = \sum_{j=1}^{2} \sum_{i=1}^{N_j} (\mu j - \mu)(\mu j - \mu)^T (7)$$

Where j = 1 represents the blurred class, j = 2 represents the sharp class, xi is the intensity of the i-th pixel, and N j is the number of pixels in the corresponding region (see also [42, Sec. 2.3]). This is solved by maximizing the ratio $\|S_w S_b\|$ and the resulting column vectors of the projection matrix W are the eigenvectors of $S_w - 1 S_b$.

The final metric can be expressed as:

$$m_{LDA}(i) = W_i^T P (8)$$

Where W_i^T is the i-th column vector of matrix W, and p is the vectorized patch intensity.

3) Sparsity:

This measure is based on sparse representation. Each patch is decomposed according to a learned over-complete dictionary which expressed as

$$arg_u^{min} \|P - Du\|^2 + \lambda \|u\|1 \quad (9)$$

Where D is the learned dictionary on a set of blur image patches. p is the vectorized patch intensity and u is the coefficients vector, each item of which is the weight used for the reconstruction. The reconstruction of a sharp patch requires more words than blurred patches. Thus the sharpness measure is defined as the number of non-zero elements in u, i.e., the L0 norm of u.

$$m_S = \|u\|1 \quad (10)$$

4) Total Variation: This metric is defined as

$$m_{TV} = \frac{1}{4} \, {}_{\xi \epsilon P}^{max} TV(\xi)$$

$$with\, TV(\xi) = \frac{1}{255}\sum_{i,j}|xi - yi| \quad (11)$$

Which is the maximum of the total variation of smaller blocks ξ (set as 2×2 in the original paper) inside the local patch P.? The coefficient 1 4 is a normalization factor since the largest TV of a 2×2 block is 4. The author argued that a non-probabilistic application of TV can be used as a measure of local sharpness due to its ability to take into account the degree of local contrast.

C. Frequency Domain Metrics

1) Power Spectrum:

The average of the power spectrum for frequency ω of an image patch is:

$$J(\omega) = \frac{1}{n}\sum_{\theta}J(\omega,\theta) \cong \frac{A}{\omega^{\alpha}} \quad (12)$$

Where $J(\omega,\theta)$ is the squared magnitude of the discrete Fourier transform of the image patch in the polar coordinate system, n is the number of quantization of θ, and A is an amplitude scaling factor. Since the power spectra of blurred regions tend to have a steeper slope than for sharp regions, thus have a smaller average power. The metric is:

$$m_{APS} = \frac{1}{n}\sum_{\omega}\sum_{\theta}J(\omega,\theta) \quad (13)$$

In [2], the authors directly use the fitted spectrum slope α as the measure. However, Ferzli and Karam claimed that the average power spectrum is more robust to outliers and overfitting, thus we only evaluate m APS.

D. Response Behavior of Sharpness:

we assumed there are four common types of textures that appear in natural scenes, a random texture such as grass, a man-made texture, a smooth texture such as sky or fruit surface, and an almost smooth texture such as areas on the road sign (the characteristic of this texture is of low contrast and has more detail than pure smooth regions).

Four such exemplar textures are shown in Figure 1. It can be seen from this figure that, in an aggregate manner, all measures decrease when blur increases (one exception is that mK shows a slight increase after σ approaches 5). However, the aggregate data hides responses that are very different from the aggregate with mGHS and mK exhibiting minor to moderate non-monotonicity on some specific textures. Two patches are shown in Figure 3 with two levels of blur. The one with larger σ has larger mK. A smooth texture should elicit a constant, yet low response to the sharpness metrics since its appearance does not change

man-made texture   random texture

smooth texture   almost smooth texture

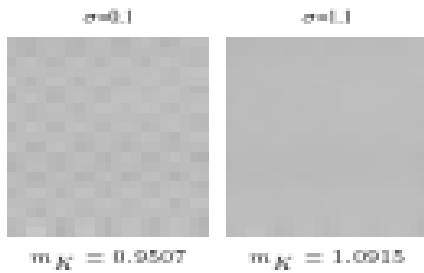Fig.1. Four commonly appeared textures in natural scenes.

Fig.2. An example of the non-monotonicity of the sharpness measure mK .

The patches showing here is the almost smooth patch under two levels of Gaussian blur as marked by black dots in mK response in Figure 2. with varying degrees of defocus blur, but the yellow curve shows big differences in responses for most of the sharpness metrics, with mGHS, mTV and mSVD exhibiting the least variation.

One would also expect that blurry regions would have smaller response than sharp regions, but that is not the case for all metrics. For example, at σ = 1.5 the range of values between the higher and lower quartile has a large overlap with range when σ = 0. This is because the low contrast region has very small intensity variance which leads to low gradient and low frequency response.

This drawback is further shown in Figure 11. The low contrast yellow region of the road sign does not have a correct response for all measures even if it is in focus. In the next section we present our new sharpness metric based on local binary patterns which is monotonic. The range of response values for blur patches has less intersection than that of sharp regions and it has a more appropriate response to low contrast region.

III. PROPOSED LBP BASED BLUR METRIC

In object recognition, segmentation of background and foreground, texture classification and identification of 3D surface characteristics, Local Binary Patterns (LBP) has been succeed.
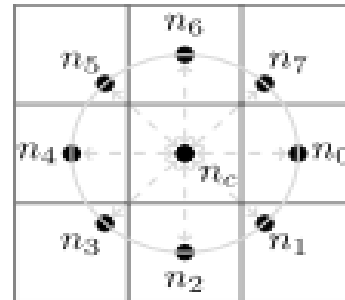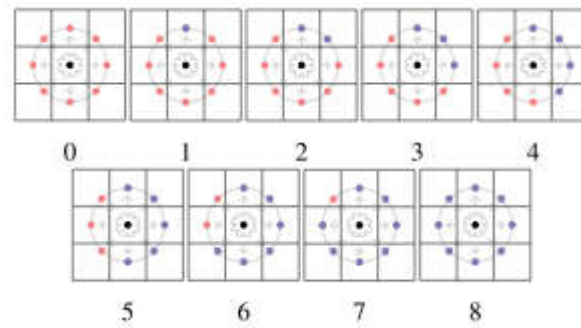

Fig.3. 8-bit LBP with P = 8, R = 1.

Fig.4. the uniform rotationally invariant LBP.

A pixel LBP code (Xc, Yc) is described as:

$$LBP_{P,R}(Xc, Yc) = \sum_{p=0}^{P-1} S(n_p - n_c) \times 2^P$$

$$with S(x) = \begin{cases} 1 & |x| \geq T_{LBP} \\ 0 & |x| < T_{LBP} \end{cases} (14)$$

Here n_c is the central pixel (Xc, Yc) intensity, n_p denotes the p neighboring pixels intensities with the radius R and those pixels are

circulated around the center n_c, and TLBP > 0 is a minimum, positive threshold in order to get robustness for flat image regions as in [19]. Figure 4 gives the n_p neighboring pixels location when R=1 and P=8.The intensity value of n_p is calculated by using the bilinear interpolation. A turn invariant adaptation of LBP can be accomplished by playing out the roundabout bitwise right shift that limits the estimation of the LBP code when it is deciphered as a binaryvalue.

By using this, pattern number is decreased to 36. According to Ojala et al., all rotation invariant patterns are not equally well in maintaining the rotation. Therefore in our proposed work we are using uniform patterns. Uniformpatterns are nothing butrotation invariant patternsubsets. A pattern is said to be uniform when the circular bit sequence has no more than two transformations i.e, zero to one or one to zero. Then all non-uniform patterns are grouped as one pattern. This single pattern additionally reduces the unique pattern number to 10.(i.e, single non-uniform pattern and remaining 9 are uniform patterns).

Figure 5 gives the uniform pattern of rotationally invariant LBP. In Figure 5, some pixels has its intensity difference from its center pixel is maximum than TLBP and some pixels has minimum than that TLBP. Maximum intensity difference pixels are coloured with blue and minimum intensity pixels are coloured with red. We can say that blue coloured pixels are 'triggered'.

0–8Bins denotesuniform pattern counts; 9thbin denotes the non-uniform pattern counts. Here we are taking the data from 100 partially blurred images.
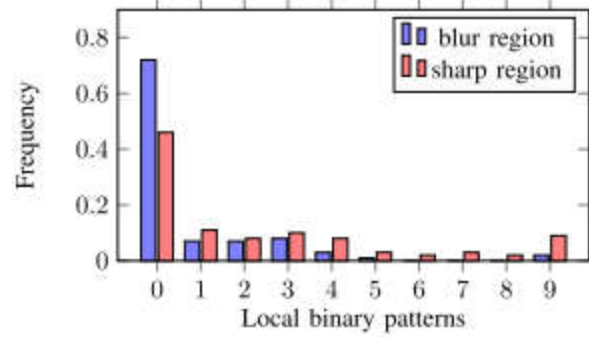

Fig.5. Distribution of LBP code in blurred and sharp regions.

Figure 6 shows the pattern histogram. These 9 uniform LBP patterns are taken from the 100 partially blurred images. 9th bin gives the non-uniform pattern number.

Our sharpness metric explores these considerations:

$$m_{LBP} = \frac{1}{n}\sum_{i=1}^{n} n\left(LBP_{8.1}^{riu2}i\right) \quad (15)$$

Here N- total No. of pixels in the selected Local region and n denotes the No. of rotation invariant uniform 8-bit LBP pattern of type I. these are mainly used to normalize the metric i.e..,$m_{LBP} \in [0,1]$.the main benefit of the system is sharpnessmeasurement in the LBP domain. This LBP features are strong to monolithic illumination changes. Mainly it occurs in natural Images. In Eq (14) threshold value TLBP reduce the proposed metric's sensitivity to sharpness. So we can observe in Fig 8 is with expanding TLBP, we can get sharpness in metric is very less precise.

By observing the Fig 9, we will get the tradeoff between two terms i.e., sharpness Precise and noise toughness. In this type of activity we should be employ a discontinuity-preserving noise removing filterlike non-local means where maximum

sensitivity to sharpness is required. We will get the plot between multiple levels of blur and our metric response in Fig 10.Compared to other metrics, the blur and sharp intersection is much smaller because of the sharp decline between the values of σ from 0.2-1.0.

If σ value reaches to greater than one, then all patches diminish to the value 'zero'. So, by utilizing simple thresholding only sharp and blur region segmentations are simplified. Furthermore, when compared to other metrics our proposed algorithm's most smooth region can bring out plenty response. At last the response of metric is monotonic as well as decreases in accordance to the automatic progressive blur. For this reason we will get greater precision and thickness in segmentation.
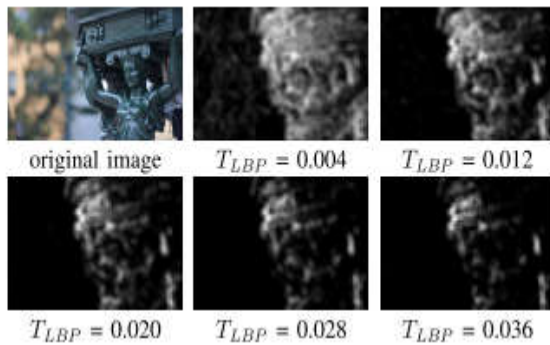
Fig.7. Response of mLBP (Equation 15) for various values of threshold TLBP.
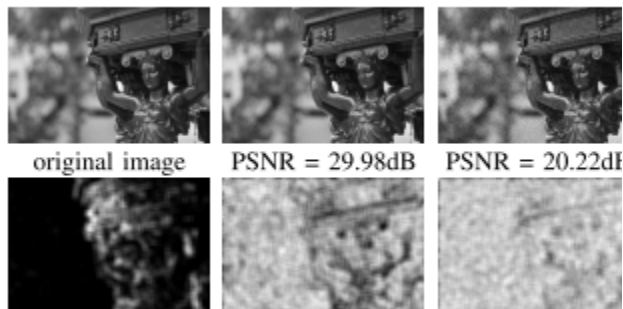
Fig.8. Response of mLBP in the presence of noise.

IV. NEW BLUR SEGMENTATION ALGORITHM

Here we discuss about ourLBP-based sharpness metric algorithm for partially blurred image segmentation.

LBP-based sharpness metric algorithm has 4 steps:

A. Generation of a map for multi scale sharpness.
B. Initialization of alpha matting
C. Estimation of Alpha map
D. Sharpness conclusion

A. Generation of a map for multi scale sharpness.

Using mLBP, here we are generating multi-scale sharpness maps. For each image pixel, sharpness metric is calculated. This metric calculation is for a local patch. Each sharpness map is build at 3 scales. Here scale is nothing but a size of local patch. At a constant P and R sharpness maps are calculated in stable time per pixel by utilizing an integral image.

B. Initialization of alpha matting

Here alpha matting means Segmentation of foreground and background regions in an image. Eq (16) provides formation model of an image,

$$I(x,y) = \alpha_{x,y}F(x,y) + \left(1 - \alpha_{x,y}\right)B(x,y) \quad (16)$$

From Eq (16) $\alpha_{x,y}$---Pixel position(x,y)opacity value, if a pixel locates in the foreground region then it may be elucidated as the determination. To mark the known pixels in foreground and background, we

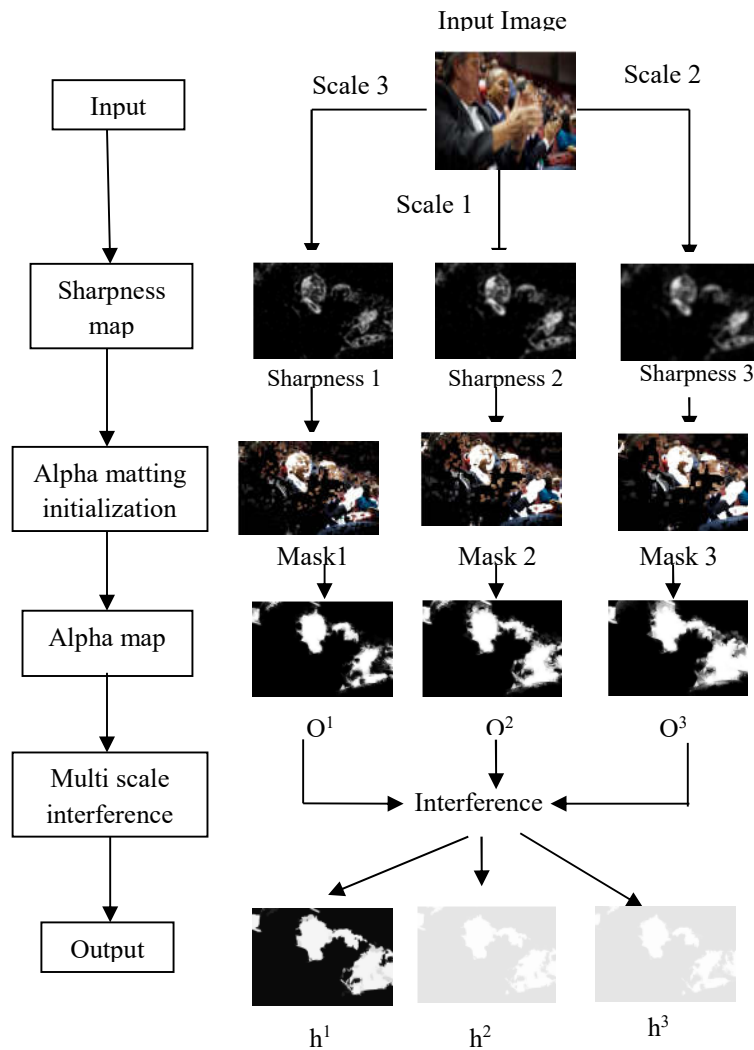are using alpha matting and foreground pixels are initialized with $\alpha = 1$. and background pixels are

Fig.12. Proposed segmentation algorithm.

initialized with $\alpha = 0$. By this, "foreground" is simply treated like a 'sharp portion' similarly, background is simply treated as 'blurred portion' .by applying a double threshold to the maps of metric sharpness ,we initialized this process automatically.

$$mask^s(x,y)$$
$$= \begin{cases} 1, & if\, m_{LBP}(x,y) > T_{m1} \\ 0, & if\, m_{LBP}(x,y) > T_{m1} \quad (\,17) \\ m_{LBP}(x,y), otherwise \end{cases}$$

Here s denotes the scale, and $mask^s(x,y)$ is nothing but introductory α-map at the scale s.

C. Estimation of Alpha map

Levin invented a below cost function. With the minimization of this cost function we can solve the α-map

$$E(\alpha) = \alpha^T L_\alpha + \lambda(\alpha - \hat{\alpha})(\alpha - \hat{\alpha})^T \text{ (18)}$$

D. Sharpness conclusion

To get the ultimate output, we adopted one multi scale graphical model. In this graphical model the total energy is described in following Eq (19)

$$E(h) = \sum_{S=1}^{3}\sum_{i}|h_i^s - \widehat{h_i^s}| + \beta\left(\sum_{S=1}^{3}\sum_{i}\sum_{j\in}|h_i^s - h_j^s| + \sum_{S=1}^{2}\sum_{i}|h_i^s - h_j^{s+1}|\right) \text{ (19)}$$

From Eq (19)

$\widehat{h_i^s} = \alpha$----map of α for scale S locates at pixel i. It is calculated in the last step

h_i^s----Implicit in sharpness.

At the right side First Term---Unary term

second term ----Pairwise term

β ----It regulates the above two terms relative importance.

By using loopy belief propagation we will optimize Eq (19).

We are taking an input image as integral image. For that image we are applying above 4 steps. By applying above 4 steps which are shown on the left side of the figure 12, we will get the required output i.e, the image after segmenting the in and out-of-

Here α denotes a vectorized α-map,$\hat{\alpha} = maski(x, y)$ --- from the previous step we can initialize the vectorized alpha maps and L denotes Laplacian matrix for matting. $(\alpha - \hat{\alpha})$ Indicates regulation term and $(\alpha - \hat{\alpha})^T$ indicates data fitting term. These terms ensures smoothness and encourages similarity to αˆrespectively. At each and every scale the last alpha map is indicated as α_s,s = 1, 2, 3.

focus blur. The above using image is grayscale image, here maximum intensity values gives greater sharpness.

EXTENSION:

The motivation of Line Local Binary Pattern (LLBP) is from Local binary pattern (LBP) due to it summarizes the local special structure (Micro-structure) of an image by thresholding the local window with binary weight and introduce the decimal number as a texture presentation. Moreover it consumes less computational cost.

The basic idea of LLBP is similar to the original LBP but the difference as follows:

1. The LLBP neighbourhood shape is a straight line with length n Pixel, unlike in LBP which is a square shape.

2. The distribution of binary weight is started from left and right adjacent pixel of center pixel to the end of left and right side.
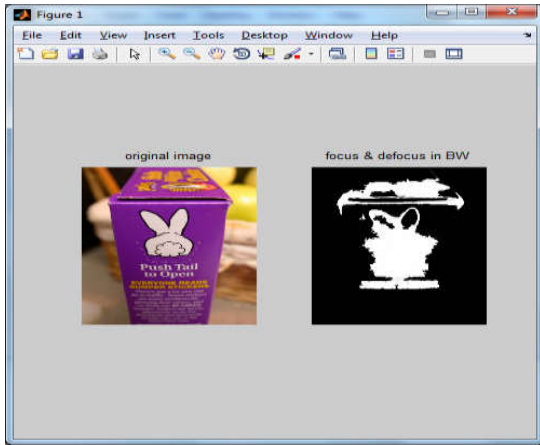
RESULTS

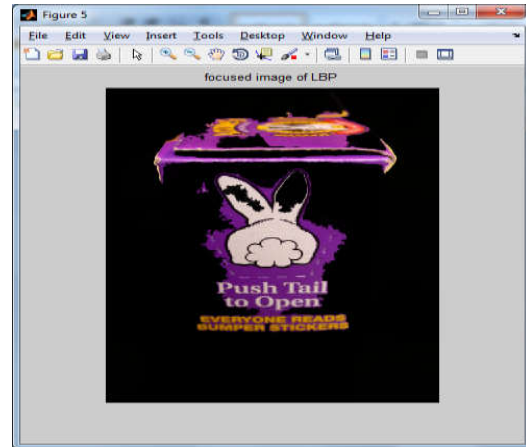Fig.1. (a) Original Image (b) focus image in BW
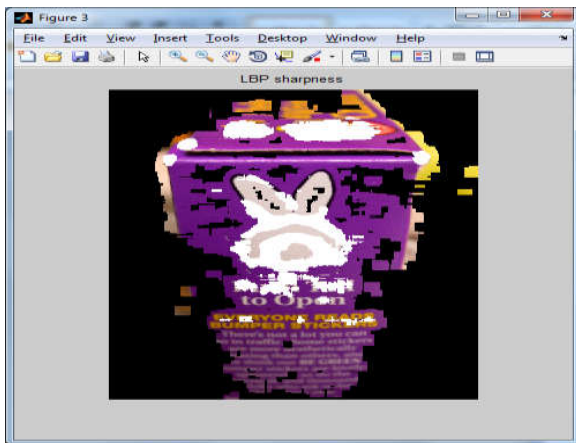

Fig.4. Focus Image
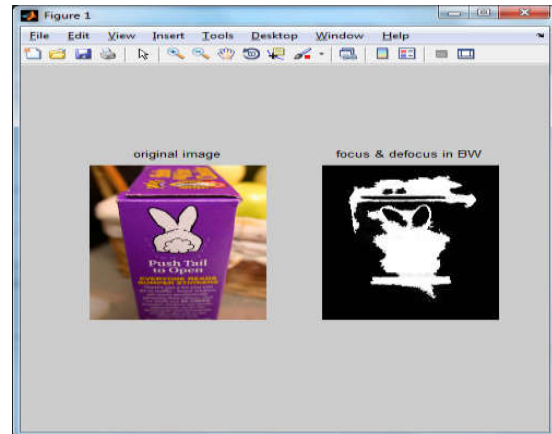

Fig.2. LBP sharpness

Fig.5. (a) Original Image (b) LLBP image in BW
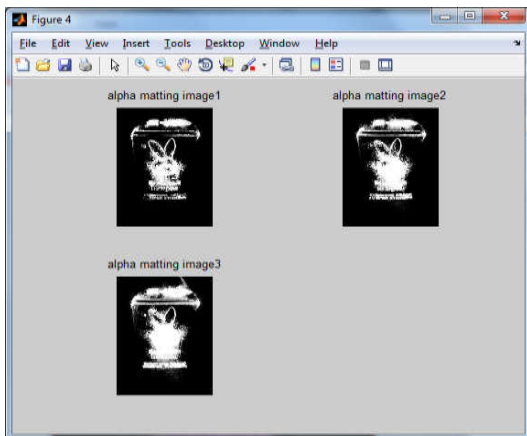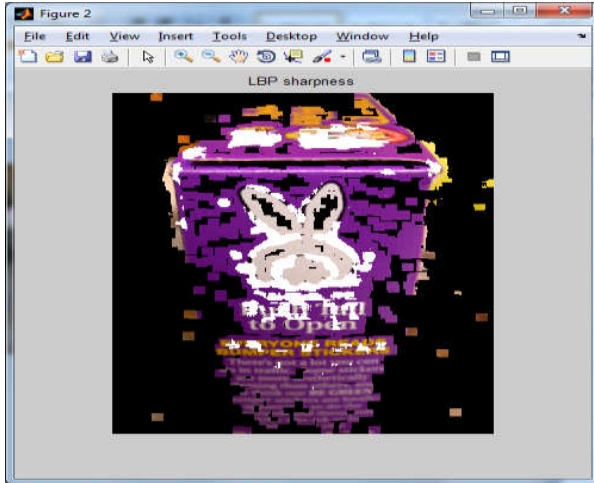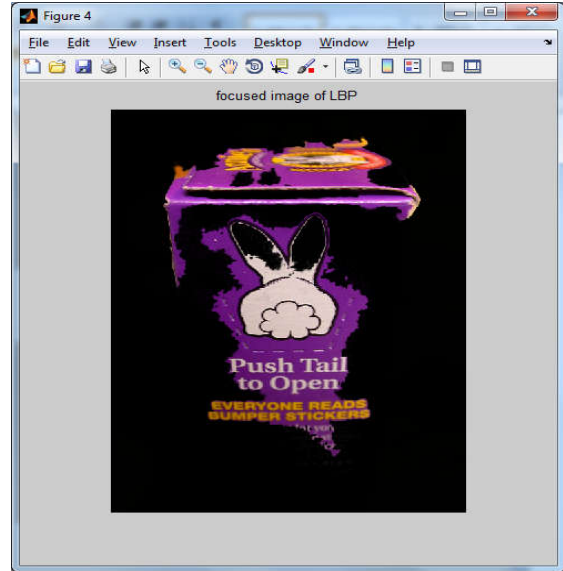

Fig.3. Alpha Matting

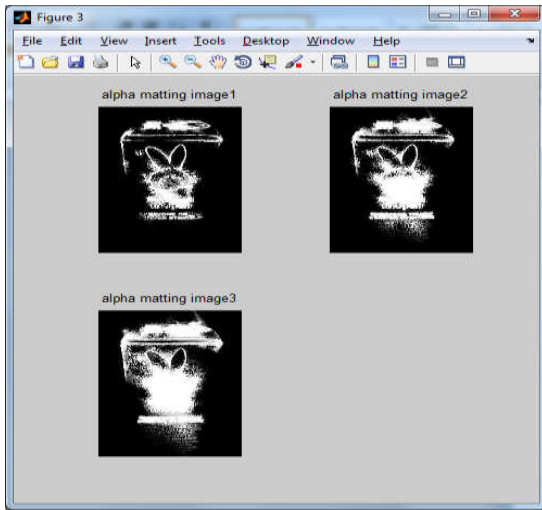Fig.6. LLBP Sharpness Image

Fig.8. Focus Image
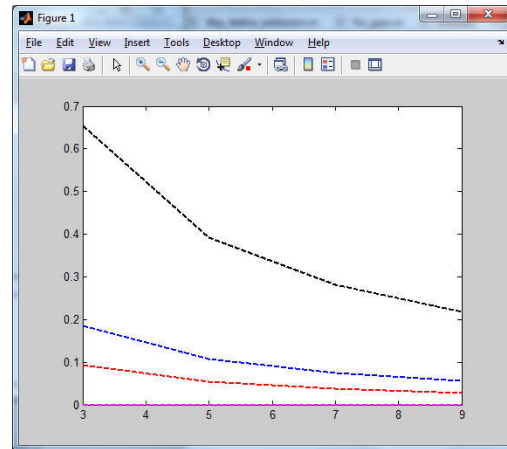

Fig.7. Alpha Matting
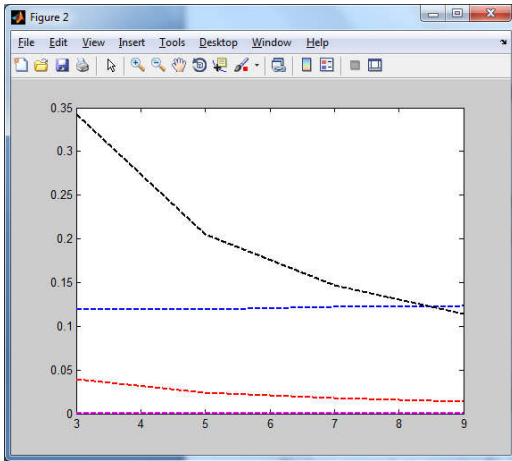

Fig.9(a). Local Kurtosis
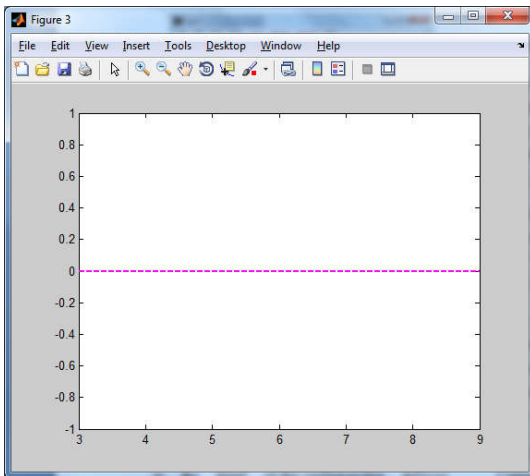
Fig.9(b) Gradient Histogram Span

Fig.9(c) Local Power Spectrum Slope

Fig.9. Responses of different measures. The thick red curve shows the mean performance over 8000 patches and the dashed red line shows the higher and lower quartile. The responses to 4 exemplar patches are shown in blur, cyan, green, grey curves respectively.

VI. CONCLUSION

We have proposed an exceptionally basic yet powerful sharpness metric for defocus blur segmentation. This metric depends on the dispersion of uniform LBP patterns in blur and non-blur image locales. The immediate utilization of the local crude sharpness measure can accomplish similar outcomes to the detail of-the-craftsmanship defocus segmentation technique that in light of meager portrayal, which demonstrates the capability of local based sharpness measures. By incorporating the metric into a multiscale data spread casing work, it can accomplish relative outcomes with the cutting edge. We have demonstrated that the calculation's execution is kept up when utilizing a naturally and adaptively chose edge Tseg.

Our sharpness metric measures the quantity of certain LBP patterns in the local neighborhood along these lines can be effectively executed by necessary images. On the off chance that joined with ongoing tangling calculations, for example, GPU usage of worldwide tangling [18], our strategy would have huge speed advantage over alternate defocus segmentation calculations.

Compare to MLBP (Multi-scale Local Binary Pattern) we get efficient results in LLBP (Line Local Binary Pattern).we can observe in Results section.

REFERENCES

[1] R. Achanta, S. Hemami, F. Estrada, and S. Susstrunk, "Repeat tuned momentous region acknowledgment," in Proc. IEEE Conf. Comput. Vis. Illustration Recognit. (CVPR), Jun. 2009, pp. 1597–1604.

[2] H.- M. Adorf, "Towards HST recovery with a space-variety PSF, cosmic bars and other missing data," in Proc. Revamping HST Images Spectra-II, vol. 1. 1994, pp. 72– 78.

[3] T. Ahonen, A. Hadid, and M. Pietikäinen, "Face depiction with neighborhood twofold illustrations: Application to face affirmation," IEEE Trans.

Illustration Anal. Mach. Intell., vol. 28, no. 12, pp. 2037– 2041, Dec. 2006.

[4] S. Bae and F. Durand, "Defocus enhancement," Comput. Outline. Talk, vol. 26, no. 3, pp. 571– 579, 2007.

[5] K. Bahrami, A. C. Kot, and J. Fan, "A novel approach for mostly cloud acknowledgment and division," in Proc. IEEE Int. Conf. Media Expo (ICME), Jul. 2013, pp. 1– 6.

[6] J. Bardsley, S. Jefferies, J. Nagy, and R. Plemmons, "A computational method for the remaking of pictures with a cloud, spatially-contrasting dark," Opt. Exp., vol. 14, no. 5, pp. 1767– 1782, 2006.

[7] A. Buades, B. Coll, and J.- M. Morel, "A non-neighborhood computation for picture denoising," in Proc. IEEE Comput. Soc. Conf. Comput. Vis. Illustration Recognit. (CVPR), vol. 2. Jun. 2005, pp. 60– 65.

[8] G. J. Burton and I. R. Moorhead, "Shading and spatial structure in consistent scenes," Appl. Select., vol. 26, no. 1, pp. 157– 170, 1987.

[9] A. Chakrabarti, T. Zickler, and W. T. Freeman, "Looking at spatially-fluctuating dark," in Proc. IEEE Conf. Comput. Vis. Illustration Recognit. (CVPR), Jun. 2010, pp. 2512– 2519.

[10] T. S. Cho, "Development darken removal from photographs," Ph.D. work, Dept. Pick. Eng. Comput. Sci., Massachusetts Inst. Technol., Cambridge, MA, USA, 2010.